

A KINETIC STUDY ON THE MASS TRANSFER WITH CHEMICAL REACTION IN THE AUC PRECIPITATION PROCESS

Hyung-Shik Shin*, Sung-Il Chung** and In-Soon Chang

Korea Atomic Energy Research Institute
(Received 16 April 1991 • accepted 29 June 1992)

Abstract—The theoretical analysis of mass transfer with chemical reaction kinetics is developed for AUC precipitation process using the penetration theory and computed numerically on an VAX 11/780. The nonlinear partial differential equations were solved by a finite difference method of Crank-Nicolson. Approximate solutions can be used to study experimental parameters and to interpret the experimental results in AUC precipitation process.

INTRODUCTION

The sinterable UO_2 powder has been widely used in nuclear power plants nowadays, which is mainly manufactured by either dry or wet processes. One of the wet processes is the ammonium uranyl carbonate (AUC) process developed at KWU-RBU in Germany. In this process carbon dioxide and ammonia gases are initially injected into demineralized water through jet at room temperature and atmospheric pressure. A pump is used to circulate the solution containing the gases and to enhance mixing process in the reactor. The solution temperature is raised up to $60^\circ C$ using a heating system and the necessary amount of uranyl nitrate (UNH) solution is fed into the precipitator.

The dissolved UNH reacts with the hydrated NH_3 and CO_2 , and yellow colored AUC crystals in monoclinic form are precipitated. This intermediate product AUC crystal is further converted into UO_2 powder through a redox process in a fluidized bed. At this stage, characteristics of UO_2 powder are predetermined [1] by the AUC precipitation. Nevertheless, the information of reaction mechanisms is not available, so it is very difficult to interpret the experimental results of the AUC precipitation process. The objective of this work is to investigate the reaction mechanism for the AUC precipitation and furthermore to charac-

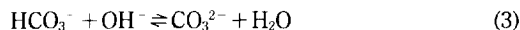
terize the AUC precipitation process.

THEORETICAL MODELLING

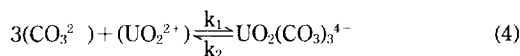
The problem to be considered first is that in which gaseous species CO_2 and NH_3 dissolve into an aqueous phase and then dissociate into the following equations:



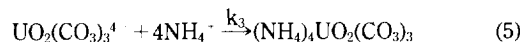
Since carbon dioxide is a weak acid and ammonia a weak base, additional ionic equilibrium must be considered:



Now, we can treat CO_3^{2-} and NH_4^+ as reactants and assume that the species CO_3^{2-} first diffuses into an interface between UO_2^{2+} and surrounding water molecules and then reacts with UO_2^{2+} as follow:



Uranyl carbonate, $UO_2(CO_3)_3^{4-}$ is formed instantaneously [4] and irreversibly reacts with the surrounding hydrated ammonium ions to form nuclei of AUC by the following reaction mechanism:



Since the fluid is continuously circulated with the injected gases, it is appropriate to use the penetration theory of Higbie for an analysis of the diffusion mech-

*Dept. of Chem. Eng., Chonbuk National University, Chonju, Chonbuk 560-756, Korea

**Dept. of Microbiology, University of Illinois at Chicago, 835 S. Wolcott Ave., Chicago, Illinois 60612, U.S.A.

anism with chemical reaction. First, it is considered that one reactant diffuses into a semi-infinite medium containing a second reactant that depletes the first by the known kinetic mechanism. Presently, Eqs. (4) and (5) are considered for the analysis of mass transfer with chemical reactions.

It is assumed that during a short period of contact time, liquid is completely and instantaneously mixed while being circulated through pumping, thus, each component has a flat concentration profile. The contact time between successive mixing is so short that the absorbing species penetrate deeply enough, so the liquid depth is assumed to be infinite for the mathematical simplicity [2].

MATHEMATICAL REPRESENTATION

One can write the following differential equations for each species:

$$D_A \frac{\partial^2 A}{\partial x^2} = \frac{\partial A}{\partial t} + (k_1 A^\alpha \cdot B^\beta - k_2 M^\gamma) \tag{6}$$

$$D_B \frac{\partial^2 B}{\partial x^2} = \frac{\partial B}{\partial t} + (k_1 A^\alpha \cdot B^\beta - k_2 M^\gamma) \tag{7}$$

$$D_M \frac{\partial^2 M}{\partial x^2} = \frac{\partial M}{\partial t} + (k_2 M^\gamma - k_1 A^\alpha \cdot B^\beta) + k_3 M^\gamma \cdot C^\delta \tag{8}$$

$$D_C \frac{\partial^2 C}{\partial x^2} = \frac{\partial C}{\partial t} + k_3 M^\gamma \cdot C^\delta \tag{9}$$

where A, B, M and C refer to CO₃²⁻, UO₂²⁺, UO₂(CO₃)₃⁴⁻, and NH₄⁺, respectively. The boundary conditions to be imposed on the simultaneous solutions of these partial differential equations are

$$\begin{aligned} \text{at } t=0, x>0; \quad & A=0 \\ & B=B_o \\ & C=0 \\ & M=0 \end{aligned} \tag{10}$$

$$\begin{aligned} \text{at } t=0, x=0; \quad & A=A_i \\ & \frac{\partial B}{\partial x} = 0 \\ & C=C_i \\ & \frac{\partial M}{\partial x} = 0 \end{aligned} \tag{11}$$

$$\begin{aligned} \text{at } t>0, X \rightarrow \infty; \quad & A=0 \\ & B=B_o \\ & C=0 \\ & M=0 \end{aligned} \tag{12}$$

where subscripts i and o represent the interfacial and

the bulk concentrations of species respectively. A typical local concentration profile around the gas-liquid interface of each chemical species is shown in Fig. 2. Using the following dimensionless forms, the resulting equations become:

$$\frac{\partial^2 a}{\partial y^2} = \frac{\partial a}{\partial \theta} + (a^\alpha \cdot b^\beta - pm^\gamma) \tag{13}$$

$$r_b \frac{\partial^2 b}{\partial y^2} = \frac{\partial b}{\partial \theta} + (q_1 \cdot a^\alpha \cdot b^\beta - q_2 m^\gamma) \tag{14}$$

$$r_m \frac{\partial^2 m}{\partial y^2} = \frac{\partial m}{\partial \theta} + (q_3 m^\gamma - a^\alpha \cdot b^\beta) + q_4 m^\gamma \cdot c^\delta \tag{15}$$

$$r_c \frac{\partial^2 c}{\partial y^2} = \frac{\partial c}{\partial \theta} + q_5 m^\gamma \cdot c^\delta \tag{16}$$

where

$$\begin{aligned} p &= k_2/k_1 \cdot A_i^{\gamma-\alpha} \cdot B_o^{-\beta} = q_2/q_1 \\ q_1 &= A_i/B_o \\ q_2 &= k_2/k_1 \cdot (A_i^{\gamma-\alpha+1}/B_o^{\beta+1}) = p \cdot q_1 \\ q_3 &= p \\ q_4 &= k_3/k_1 \cdot A_i^{\gamma-\alpha} \cdot B_o^{\delta-\beta} \\ q_5 &= q_4 \cdot A_i/B_o = q_4 \cdot q_1 \end{aligned}$$

and the dimensionless variables and constants are:

$$\begin{aligned} a &= A/A_i \\ b &= B/B_o \\ c &= C/B_o \\ m &= M/A_i \\ A_i &= 1.13 \\ y &= \sqrt{\frac{k_1 B_o^\beta \cdot A_i^{\alpha-1}}{D_A}} x \\ \theta &= k_1 B_o^\beta \cdot A_i^{\alpha-1} \cdot t \\ K &= k_1/k_2 = 10^{18.3}; \quad k_1 = 1.0 \times 10^{-3} \text{ [3]} \\ r_b &= D_B/D_A = 0.28 \\ r_m &= D_M/D_A = 0.28 \\ r_c &= D_C/D_A = 1.19 \end{aligned}$$

It is convenient to have the relationship between the mass transfer rate with and without reaction. From the method of Secor and Beutler [4], the ratio of the average rate of diffusion accompanied by chemical reaction to that of physical diffusion for species CO₃²⁻ was obtained [3].

$$\Phi = \frac{K_L}{K_L^*} = \frac{1}{2(1-a_o)} \sqrt{\frac{\pi}{\theta}} \int_0^\infty \left[a - a_o + \frac{q_1(1-b)}{r_b} \right] dy \tag{17}$$

where

$$\begin{aligned} K_L^* &= 2(1-a_o) \sqrt{\frac{k_1 B_o^\beta \cdot A_i^{\alpha+1} D_A}{\pi \theta}} \\ a_o &= A_o/A_i \end{aligned} \tag{18}$$

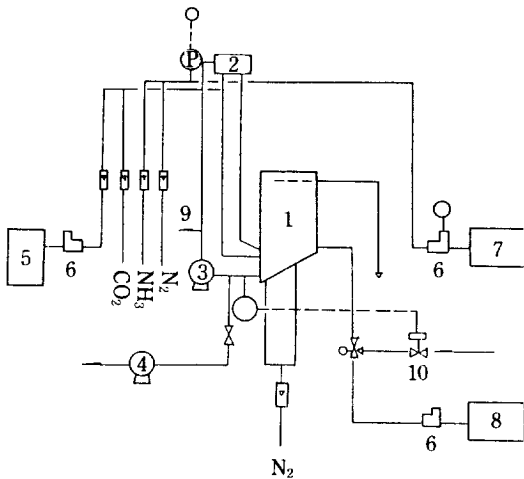


Fig. 1. Schematic diagram of experimental apparatus.

- 1. Reactor
- 2. Mixing nozzle box
- 3. Pump
- 4. Product pump
- 5. UNH storage
- 6. UNH feeding pump
- 7. Demineralized water tank
- 8. Hot water tank
- 9. Sampling tap
- 10. Solenoid valve
- P. Pressure indicator

NUMERICAL PROCEDURES

The above Eqs. (13) through (16) are nonlinear partial differential equations and can not be solved analytically. Numerical procedures, however, for such problems have been successfully applied to get approximate solutions. In the work, a finite difference with the Crank-Nicolson method was used:

$$a_j^{k-1} = a_j^k + 1/2 \left[\frac{da_j^k}{d\theta} + \frac{da_j^{k+1}}{d\theta} \right] \Delta\theta \tag{19}$$

$$\frac{da_j^k}{d\theta} = \frac{\partial^2 a_j^k}{\partial y^2} - [(a_j^k)^\alpha (b_j^k)^\beta - p(m_j^k)^\gamma] \tag{20}$$

$$\text{also, } \frac{\partial^2 a_j^k}{\partial y^2} \approx \frac{a_{j-1}^k - 2a_j^k + a_{j+1}^k}{\Delta y^2} \tag{21}$$

where the superscript k refers to the time increment $\Delta\theta$ and the subscript j refers to the space increment Δy , it is found that

$$a_j^{k-1} - \frac{R}{2}(a_{j-1}^{k-1} - 2a_j^{k-1} + a_{j+1}^{k-1}) = a_j^k + \frac{R}{2}(a_{j-1}^k - 2a_j^k + a_{j+1}^k) - \frac{\Delta\theta}{2} F_j^k \tag{22}$$

where $R = \Delta\theta/\Delta y^2$ and $F_j^k = 3[(a_j^k)^\alpha (b_j^k)^\beta - p(m_j^k)^\gamma]$

Here we neglect the term F_j^{k+1} for simplicity. Similar-

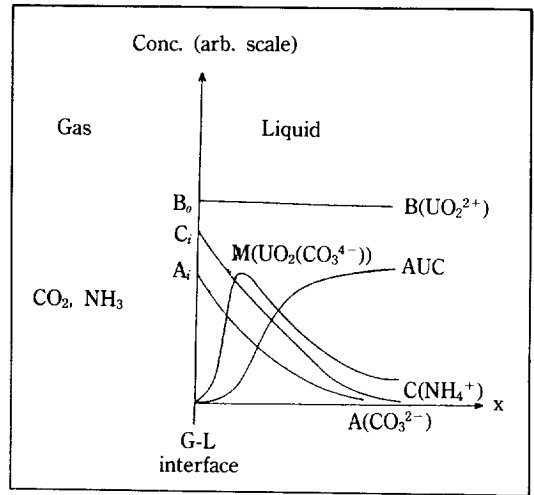


Fig. 2. Local concentration profiles around the gas-liquid interface of each component, A, B, C, and M.

ly, Eqs. (14) through (16) can be expressed in the same way.

Since F_j^k is a function of a_j^k , b_j^k , m_j^k , the j-th components of a_j^k , b_j^k , and m_j^k should be determined first. The initial boundary conditions were used to calculate F_j^k , and for the (k + 1) term of a_j^{k+1} the latest values of a_j^k , b_j^k , and m_j^k were substituted to the old data by solving sequentially for a, b, and m. The boundary conditions are:

$$\text{at } \theta=0, y>0; a_j^k = 0 \tag{23}$$

$$b_j^k = 1$$

$$c_j^k = 0$$

$$m_j^k = 0$$

$$\text{at } \theta=0, y=0; a_j^k = 1 \tag{24}$$

$$b_j^k = \frac{18b_{j-1}^k - 9b_{j+2}^k + 2b_{j+3}^k}{11}$$

$$c_j^k = C_i/B_o$$

$$m_j^k = \frac{18m_{j-1}^k - 9m_{j+2}^k + 2m_{j+3}^k}{11}$$

Eq. (22) represents a set of j simultaneous algebraic equations, which are tridiagonal in form. Algorithms were followed by Carnahan et al's method [5]. The integral term in Eq. (17) was solved by the Simpson's rule.

EXPERIMENTAL PROCEDURES

Experimental set up for this work is shown in Fig. 1. The reactor was made of two acryl slabs of 2 inches wide, 30 inches high and with an inclination of approximately 30 degrees at the bottom. Initially about 3

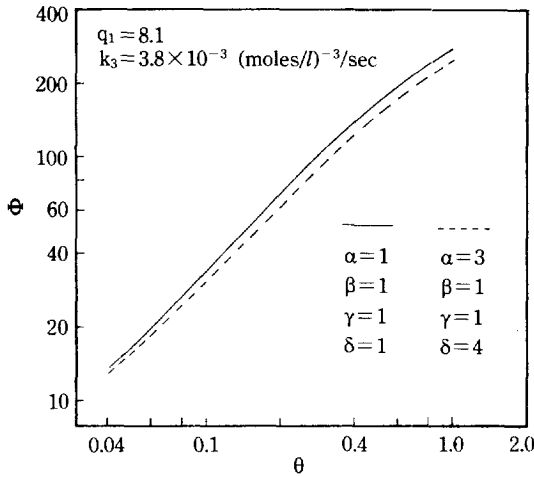


Fig. 3. Effect of chemical reaction on the mass transfer rate of CO_3^{2-} at $k_3 = 3.8 \times 10^{-3}$ (moles/liter) $^{-3}$ /sec.

liters of demineralized water was pumped into the reactor and an excess amount of CO_2 and NH_3 gases were then injected through two nozzles while circulating hot water through water jacket. Nitrogen gas was also introduced to enhance mixing of gases in the reactor. The UNH solution was then supplied as the temperature of the reactor reaches 55°C and it was thereafter kept constant by circulating cold water through water jacket to avoid temperature increase due to exothermic chemical reaction.

During the course of reaction, a small amount of sample was withdrawn and transferred to the titration solution kept at the same temperature in order to monitor NH_4^+ , CO_3^{2-} , or UO_2^{2+} ion concentrations in the solution. NH_4^+ or CO_3^{2-} concentrations were determined with two selective electrode probes (manufactured by Orion Co.) and UO_2^{2-} ion concentration by spectrophotometric technique using Asenazo-3 coloring material.

RESULTS AND DISCUSSION

The numerical results, expressed in Φ vs. θ , were obtained for the various physical parameters. Fig. 3 shows the effect of chemical reaction on the mass transfer rate of CO_3^{2-} as a function of dimensionless time. Two different values for the reaction kinetic orders were compared for the condition of $q_1 = 8.1$ and $k_3 = 3.8 \times 10^{-3}$ (moles/l) $^{-3}$ /sec. It is noticed that as the dimensionless time decreases, Φ approaches to unity in both cases and the mass transfer rate is slightly

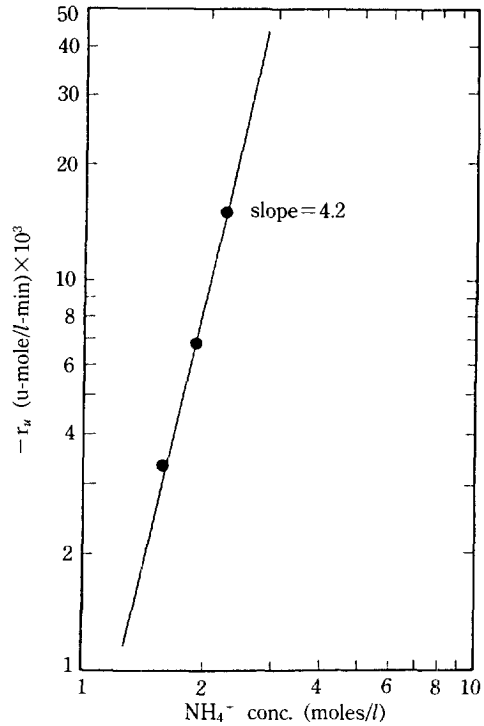


Fig. 4. Plot of reaction rate of Eq. (5) vs. NH_4^+ concentration showing the order of reaction, $\delta = 4.2$.

higher at lower reaction order than that at higher one. However, as the dimensionless time increases, the difference becomes a little larger.

The reaction rate constant, k_3 and reaction order, δ , of Eq. (5) were experimentally determined by monitoring NH_4^+ concentration in the solution which contained the excess amount of $\text{UO}_2(\text{CO}_3)_3^{4-}$ [6]. Fig. 4 shows a log-log plotting of the reaction rate of Eq. (5) vs. NH_4^+ concentration. The δ value was found to be 4.2 from the slope which is in good agreement with the model assumption of 4 and the k_3 value was calculated from the ordinate intercept and the $\text{UO}_2(\text{CO}_3)_3^{4-}$ value of 0.2 g-mole/l to give approximately 3.8×10^{-3} (mol/l) $^{-3}$ /sec.

To examine the effect of feed ratio change on the chemical reaction rate in AUC precipitation process, the molar ratio of $\text{CO}_3^{2-}/\text{UO}_2^{2+}$ in the feed stream was varied. The results are summarized in Fig. 5. It is noticed that the mass transfer rate and the chemical reaction rate of CO_3^{2-} become equilibrated instantaneously and slightly increase up to its final asymptotic value at $q_1 = 1$. As the feed ratio becomes higher, the reaction rate surpassed over the mass transfer rate within the range of $\theta = 1$.

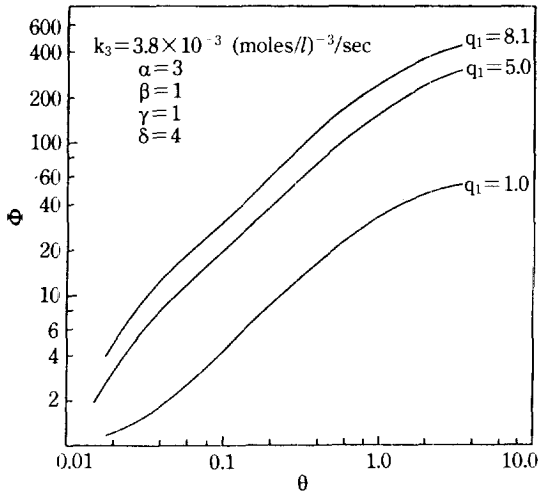


Fig. 5. Effect of feed stream ratio, q_1 on the chemical reaction rate of CO_3^{2-} .

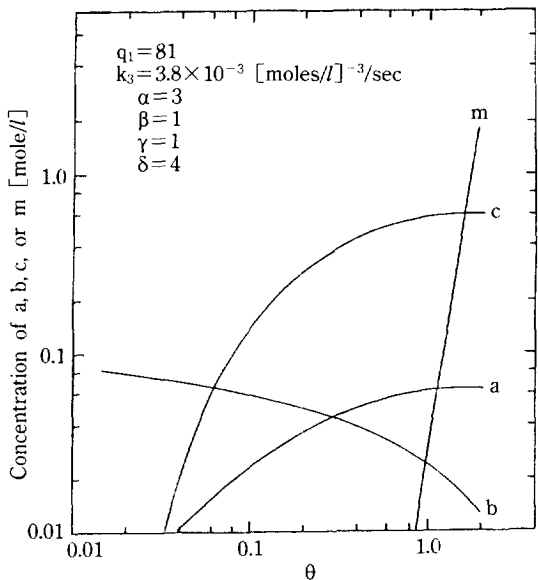


Fig. 6. Concentration changes of each component a, b, c, and m at penetration depth.

Fig. 6 shows the concentration variation of each component at penetration depth of about 4 mm away from the gas and liquid interface as a function of dimensionless time. As the chemical reactions proceed, CO_3^{2-} and NH_4^+ ion concentrations were increased by the ions supplied from the chemical equilibria, and UO_2^{2+} became consumed due to chemical reaction with CO_3^{2-} . The reaction product, uranyl carbonate formed at the interface diffuses to bulk phase. The formation of uranyl carbonate is initially a very slow process, but when the reaction goes on until θ becomes unity, its rate becomes exponential. The UO_2^{2+} concentration data detected by the spectrophotometric technique was compared with the analytical result for several local points as in Fig. 7. It shows slightly higher values than the calculated values, which may be caused by the incorporation of uranyl carbonate concentration in sampling for the analysis of UO_2^{2+} concentration.

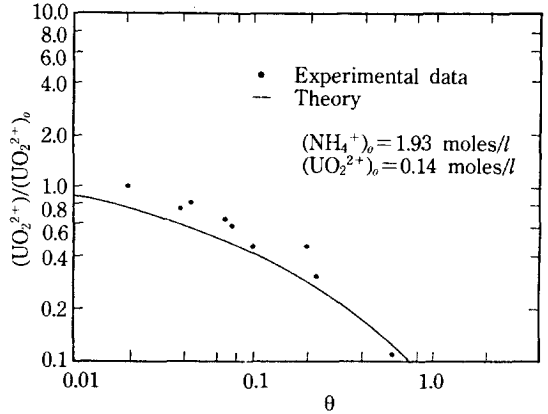


Fig. 7. Comparison of theoretical predictions with experimental data of $(\text{UO}_2^{2+})/(\text{UO}_2^{2+})_0$.

nyl carbonate is initially a very slow process, but when the reaction goes on until θ becomes unity, its rate becomes exponential. The UO_2^{2+} concentration data detected by the spectrophotometric technique was compared with the analytical result for several local points as in Fig. 7. It shows slightly higher values than the calculated values, which may be caused by the incorporation of uranyl carbonate concentration in sampling for the analysis of UO_2^{2+} concentration.

CONCLUSION AND RECOMMENDATION

Theoretical analysis of the mass transfer with chemical reaction mechanism for AUC precipitation process was investigated and the results can be summarized as follows:

1. The reaction kinetic order does not make much effect on the chemical reaction rate.
2. The chemical reaction rate is mainly affected by the feeding stream ratio, that is $\text{CO}_3^{2-}/\text{UO}_2^{2+}$.
3. All the analyses show that when $\theta = 1$, corresponding to 1.0 seconds, the chemical reaction rate becomes constant and reaches a steady state.
4. Also, the rate of formation of uranyl carbonate follows an exponential function.

This study is in a rudimentary stage for AUC precipitation process. Therefore, to have a more detailed analysis possible, it is suggested that the experiment should be carried out in a carefully prepared manner and also the data should be more accurate to distinguish between the subtle differences in their interpretation.

NOMENCLATURE

A : concentration of CO_3^{2-} entering the medium in which reaction occurs [moles/l]
 A_i : concentration of A at the interface [moles/l]
 A_0 : initial concentration of A [moles/l]
 a : A/A_i
 B : concentration of UO_2^{2-} reacting with A [moles/l]
 B_0 : initial concentration of B [moles/l]
 b : B/B_0
 C : concentration of NH_4^+ entering the medium in which reaction occurs [moles/l]
 C_i : concentration of C at the interface [moles/l]
 C_0 : initial concentration of C [moles/l]
 c : C/B_0
 D_A : diffusion coefficient, subscript indicating the species [cm^2/sec]
 K : k_1/k_2 = equilibrium constant
 k_1 : forward reaction rate constant in Eq. (4)
 k_2 : reverse reaction rate constant in Eq. (4)
 k_3 : reaction rate constant in Eq. (5)
 K_L : average mass transfer coefficient [cm/sec]
 K_L^* : average mass transfer coefficient in the absence of chemical reaction [cm/sec]
 M : concentration of $\text{UO}_2(\text{CO}_3)_3^{4-}$ [moles/l]
 m : M/A_i
 p : $1/KA_i^2 B_0$
 q_1 : A_i/B_0
 q_2 : $A_i^{(\gamma-\alpha+1)}/(K \cdot B_0^{\beta+1})$
 q_3 : p
 q_4 : $\frac{k_3}{k_1} \cdot A_i^{p-\alpha} \cdot B_0^{\delta-\beta}$
 q_5 : $q_4 \cdot A_i/B_0 = q_4 \cdot q_1$
 R : $\Delta\theta/\Delta y^2$
 r_b : D_B/D_A
 r_c : D_C/D_A

r_m : D_M/D_A
 t : time [sec]
 x : distance in the direction of diffusion [cm]
 y : $\sqrt{\frac{k_1 B_0^\beta \cdot A_i^{\alpha-1}}{D_A}} x$, dimensionless distance

Greek Letters

α : order of the reaction with respect to A
 β : order of the reaction with respect to B
 γ : order of the reaction with respect to M
 δ : order of the reaction with respect to C
 θ : $k_1 B_0^\beta \cdot A_i^{\alpha-1} t$, dimensionless time
 Φ : K_L/K_L^*

Superscript

k : time increment

Subscript

j : space increment

REFERENCES

1. Chang, I. S., Hwang, S. T., Park, J. H., Do, J. B., Choi, Y. D. and Lee, I. H.: KAERI/AR-20618, 1983.
2. Brian, P. L. T., Hurley, J. F. and Hasseltine, E. H.: *AIChE J.*, 7(2), 226 (1961).
3. Ciavatta, L., Ferri, D., Grimaldi, M., Palombari, R. and Salvaore, F.: *J. Inorg. Nucl. Chem.*, 41, 1175 (1979).
4. Secor, R. M. and Beutler, J. A.: *AIChE J.*, 13(2), 365 (1967).
5. Carnahan, B., Luther, H. A. and Wilkes, J. O.: "Applied Numerical Methods", New York, John Wiley & Sons, Inc., 1969.
6. Levenspiel, O.: "Chemical Reaction Engineering", New York, John Wiley & Sons, Inc., 1972.